Stochastic Resonance in Coupled Oscillator Systems with Time Delay

Seunghwan Kim,* Seon Hee Park, and H.-B. Pyo
Telecommunication Basic Research Labortary, Electronics and Telecommunications Research Institute, P.O. Box 106, Yusong-gu, Taejon 305-600, Korea
(Received 26 August 1998)

We investigate stochastic resonance in a globally coupled oscillator system with time delay. The system shows multistability of a desynchronized state and two synchronized states with different collective frequencies, which may be interpreted as multistable perception of ambiguous or reversible figures. Under the influence of a weak periodic external signal, the system exhibits a maximum in the signal-to-noise ratio at an optimum noise level—the characteristic signature of stochastic resonance. We also show stochastic resonance between two limit-cycles in the system. [S0031-9007(99)08392-1]

PACS numbers: 05.40.–a, 07.05.Mh, 42.66.Si, 87.10.+e

Synchronization of oscillators has been the topic of much recent investigation [1–3]. Recent experiments [4] showed the synchronized oscillations of neuronal activity in the visual cortex of the cat suggesting that information processing is a cooperative process of neurons. A coupled oscillator model was suggested to understand the temporal and spatial coherence of the oscillations of neuronal activity [2]. The inclusion of time delay into the system is natural in the realistic consideration of finite transmission of interaction. Recently, it was shown that the coupled oscillator system with time delay exhibits multistability of synchronized and desynchronized states [5]. In the synchronized state, the system has also two limit-cycles with different collective frequencies; one is larger than the intrinsic frequency and the other is smaller than the intrinsic frequency. This multistability was interpreted as the perception of ambiguous or reversible figures. Perception of the ambiguous or reversible figures is characterized by noisy multistable dynamics, that is, the different interpretations of the figures are switched with a stochastic time course [6]. Recently, there have been studies on the noisy multistable dynamics in connection with the development of dynamical models of brain function during such switchings in perception [7].

There has also been a growing interest in stochastic resonance (SR) associated with noisy nonlinear dynamical systems [8]. SR is characterized by the optimization of the response of the system to an input signal as a function of the input noise strength. The response of the system is measured by a signal-to-noise ratio (SNR) which shows a peak as a function of the input noise strength. This implies that noise may enhance the transmission of information. SR has been demonstrated in numerous physical experiments such as electronic trigger circuits [9], two-mode ring lasers [10], and mammalian neuronal networks [11]. The possible importance of SR for the processing of information in neural systems seems evident at all levels of information processing. Indeed, it has long been recognized that noise can improve the performance of certain neural networks [12], and that an optimum noise level can achieve the maximum improvement. SR in low dimensional dynamical systems with attractors is by now a familiar phenomenon, but SR in spatially distributed systems or the systems with limit cycles remains the focus of current research.

In this Letter, we investigate SR in the globally coupled oscillator system with time delay. We choose the parameter values with which the system shows multistability of a desynchronized state and two synchronized states with different collective frequencies. We apply a weak periodic external signal to the system, and measure SNR as a function of the input noise strength showing a peak at an optimum noise strength: the characteristic signature of SR. We also investigate SR in the system with time-delayed self-interaction which shows the bistability of limit cycles.

A system of N globally coupled oscillators under study is described by the equation of motion

$$\frac{d\phi_i(t)}{dt} = \omega - b\sin[\phi_i(t)] - \frac{K}{N}\sum_{j=1}^{N}\sin[\phi_i(t) - \phi_j(t-\tau)], \quad (1)$$

where ϕ_i, $i = 1, 2, \ldots, N$, is the phase of the ith oscillator. ω is an intrinsic frequency that is uniformly given to each oscillator. The sum in Eq. (1) runs over all oscillators describing the time-delayed interaction which depends on the phase difference of two oscillators with delay time τ. The second term on the right-hand side of Eq. (1) represents the pinning force introduced to mimic the dynamics of limit-cycle oscillators or excitable elements [13–15]. Here, we choose the parameter values of the system as $\omega = 1$, $b = 0.5$, $K = 1$, and $\tau = 3$ with which the system shows the multistability of a desynchronized state and two synchronized states with different collective frequencies [5].

To investigate SR in the system we apply the weak periodic signal to the system in the presence of additive

 0031-9007/99/82(8)/1620(4)$15.00

noises obtaining the stochastic differential equation

$$\frac{d\phi_i(t)}{dt} = \omega - b\sin[\phi_i(t)] - \frac{K}{N}\sum_{j=1}^{N}\sin[\phi_i(t) - \phi_j(t-\tau)] + \epsilon\sin(\Omega t) + \xi_i(t), \quad (2)$$

where ϵ and Ω are the amplitude and frequency of the signal, respectively. In Eq. (2) $\xi_i(t)$'s are independent Gaussian white noises characterized by

$$\langle \xi_i(t)\rangle = 0,$$
$$\langle \xi_i(t)\xi_j(t')\rangle = 2D\delta_{ij}\delta(t-t'),$$

where $\langle\cdots\rangle$ means an ensemble average over $\xi_i(t)$'s. D measures intensity of the additive noises $\xi_i(t)$'s. Here, we consider the signal with $\epsilon = 0.2$, which does not induce the transition among the multistable states in the absence of noise, for various values of Ω.

When $N = 1$, the stochastic equation (2) describes the motion of an oscillator with self-interaction delayed by τ exhibiting bistability of limit cycles with different frequencies when $\epsilon = D = 0$. In Fig. 1(a), we show $w_{\rm av}(t)$, average of $\frac{d\phi}{dt}$ over time interval $\Delta t = 0.1$ at time t, for the limit cycles obtained from different initial conditions. Figure 1(a) exhibits bistability of fast and slow moving states with frequencies $\omega_f \equiv 1.748$ and $\omega_s \equiv 0.235$, respectively. In Fig. 1(b), we show $\omega_{\rm av}(t)$, average of $\frac{d\phi}{dt}$ over time interval $\Delta t = 10$, for the oscillator with $\Omega = 0.01$ at $D = 0.08$. Figure 1(b) exhibits coherent transitions between the limit cycles to the signal applied to the oscillator with a missing transition at $t \sim 2700$.

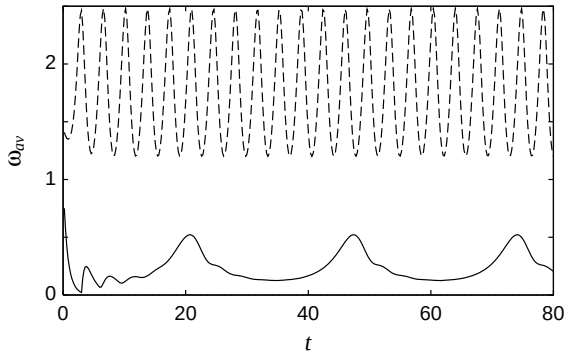

(a)

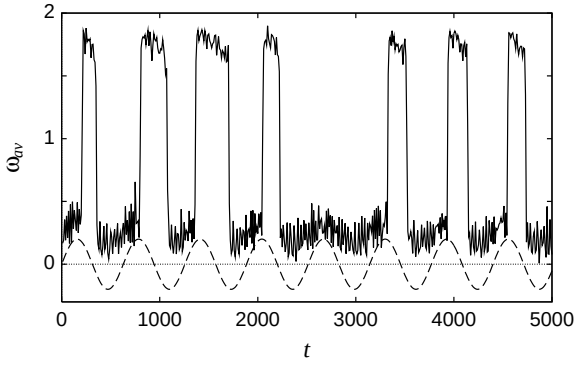

(b)

FIG. 1. Plot of time evolutions of $\omega_{\rm av} \equiv \langle\frac{d\phi}{dt}\rangle$ averaged over time interval (a) $\Delta t = 0.1$ for the system with $N = 1$ and $\epsilon = D = 0$ and (b) $\Delta t = 10$ for the system with $N = 1$, $\epsilon = 0.2$, $\Omega = 0.01$, and $D = 0.08$. Solid and dashed lines in (a) represent two stable limit-cycles with frequencies $\omega_s = 0.235$ and $\omega_f = 1.748$, respectively. Dashed line in (b) indicates the signal and solid line in (b) represents the response to the signal.

Here, we introduce the state function of the oscillator as

$$G(t) \equiv \theta(\omega_{\rm av}(t) - \omega),$$

which characterizes whether the oscillator is in the fast moving state with $\omega_{\rm av} > \omega$ or the slow moving state with $\omega_{\rm av} < \omega$ presenting 1 and 0, respectively. In the state function $G(t)$, the modulation of the response due to the input signal modulation is removed. To measure output signal intensity we calculate the power spectrum of $G(t)$. Figure 2 shows the power spectrum for the oscillator with $\Omega = 0.01$ at $D = 0.1$ exhibiting peaks at the signal frequency Ω and the multiples of the signal frequency 2Ω and 3Ω.

To observe SR in the system we calculate SNR from the usual formula,

$$\mathrm{SNR} = 10\log_{10}\left[\frac{S}{N(\Omega)}\right]$$

in dB, where S is the output signal strength given by the area under the fundamental peak in the power spectral density and $N(\Omega)$ is the noise level at the fundamental frequency. The results for the oscillator with three different signal frequencies are shown in Fig. 3 exhibiting a peak at an optimum noise level; the characteristic signature of SR.

To investigate SR in the N globally coupled oscillator system we characterize the state of the system calculating

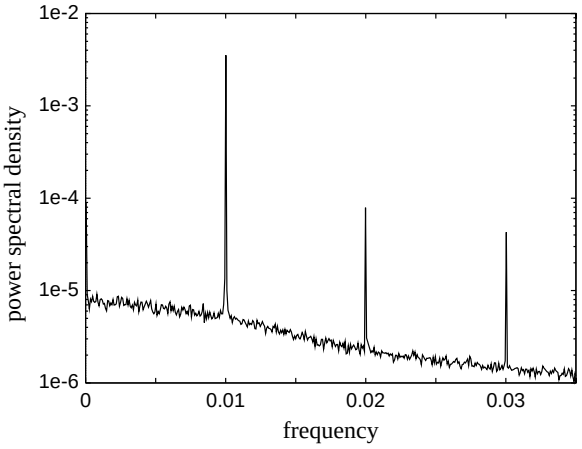

FIG. 2. Plot of power spectrum of the time series of the state function $G(t)$ for the system with $N = 1$, $\epsilon = 0.2$, $\Omega = 0.01$, and $D = 0.1$.

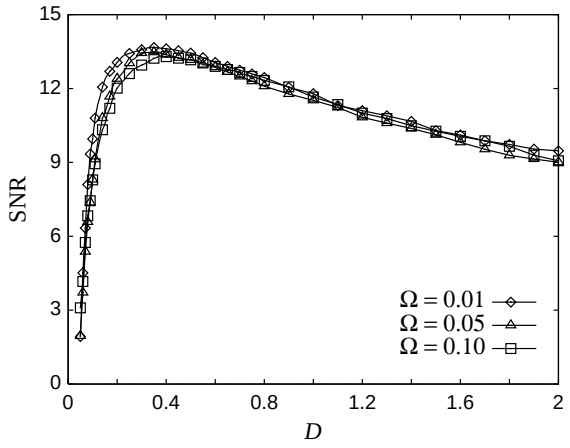

FIG. 3. Plot of SNR as a function of D for the system with $N = 1$, $\epsilon = 0.2$, and $\Omega = 0.01$ ($\diamond$), 0.05 ($\triangle$), and 0.1 ($\square$). Lines are merely guides to the eyes.

the correlation function $C(t)$ defined by

$$C(t) = \frac{2}{N(N-1)} \sum_{(ij)} \cos\langle \phi_i(t) - \phi_j(t) \rangle ,$$

where the summation is over all pairs of oscillators. $C(t)$ presents 1 for the perfectly synchronized state and 0 for the perfectly desynchronized state. In Fig. 4, we show $C_{\rm av}(t)$ and $\omega_{\rm av}(t)$, averages of $C(t)$ and $\frac{d\phi}{dt}$ over time interval $\Delta t = 10$, for the system with $N = 10$, $\epsilon = 0.2$, and $\Omega = 0.01$ at $D = 0.08$. Figure 4 exhibits three states of the system denoted by F, S, and U which represent the fast moving synchronized state, slow moving synchronized state, and desynchronized state, respectively. The states are characterized by the following conditions.

$$F\colon \omega_{\rm av} > \omega \quad \text{and} \quad C_{\rm av} \sim 1 ;$$
$$S\colon \omega_{\rm av} < \omega \quad \text{and} \quad C_{\rm av} \sim 1 ;$$
$$U\colon \omega_{\rm av} \sim \omega \quad \text{and} \quad C_{\rm av} \sim 0 .$$

Figure 4 also shows transitions among the three states correlated with the signal applied to the system.

To remove the modulation of the response due to the input signal modulation we introduce the state function of the system as

$$G_N(t) = \mathrm{sgn}(\omega_{\rm av}(t) - \omega)\theta(C_{\rm av}(t) - 0.4) ,$$

which presents 0, 1, and -1 for U, F, and S states, respectively. The power spectrum of $G_N(t)$ for the system with $N = 10$, $\epsilon = 0.2$, and $\Omega = 0.1$ at $D = 0.1$ is shown in Fig. 5 exhibiting peaks at the signal frequency Ω and the multiples of the signal frequency 2Ω and 3Ω. The broad peak at 3Ω comes from the existence of the transient U state inserted in the transition between S and F states. Figure 6 shows SNR as a function of D for various system sizes with $\epsilon = 0.2$ and $\Omega = 0.1$ exhibiting peaks at optimum noise levels; characteristic signature of SR. As N increases, the width of the peak in SNR decreases approaching a finite value in the limit of $N \to \infty$.

Figure 6 also shows the fast increase of SNR at small D and the slow decrease of SNR at large D. While the fast increase of SNR at small D results from the interplay of the noise and the input signal, the slow decrease of SNR at large D comes from the pure stochastic switchings among the multistable states, F, S, and U by the noise. The pure stochastic switchings are present even in the absence of the input signal at large D. As the noise intensity increases, the pure stochastic switching frequency also increases, leading to the slow decrease of SNR at large D. As N increases the pure noise effect decreases due to self-averaging, i.e., the cooperation of independent noises at the

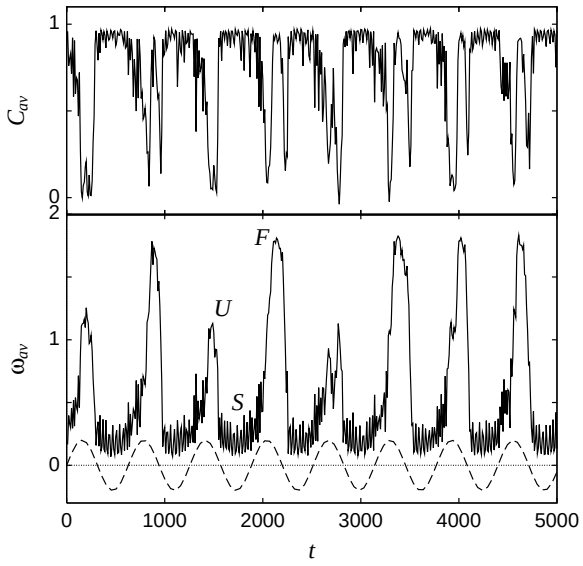

FIG. 4. Plot of time evolutions of $C_{\rm av}$ and $\omega_{\rm av}$ averaged over time interval $\Delta t = 10$ for the system with $N = 10$, $\epsilon = 0.2$, $\Omega = 0.01$, and $D = 0.08$. Dashed line represents the signal applied to the system. F, S, and U indicate the fast moving synchronized state, slow moving synchronized state, and desynchronized state, respectively.

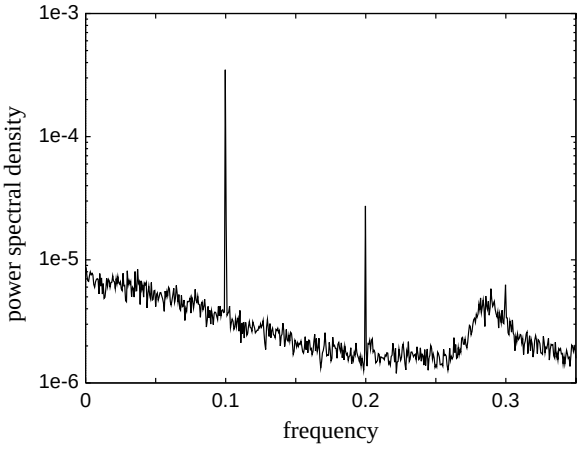

FIG. 5. Plot of power spectrum of the time series of the state function $G_N(t)$ for the system with $N = 10$, $\epsilon = 0.2$, $\Omega = 0.1$, and $D = 0.1$.

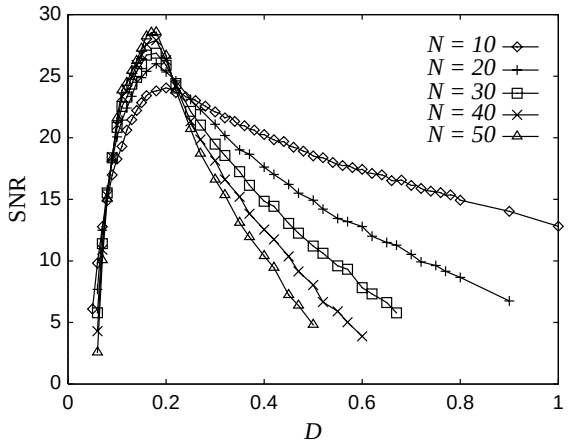

FIG. 6. Plot of SNR as a function of D for the system with $\epsilon = 0.2$, $\Omega = 0.1$, and $N = 10$ ($\diamond$), 20 ($+$), 30 ($\square$), 40 ($\times$), and 50 ($\triangle$). Lines are merely guides to the eyes.

different oscillators reduces the pure stochastic switchings. This results in the narrowing of the width of the peak in SNR as N increases. In the limit of $N \to \infty$, the self-averaging removes the pure stochastic switching, leaving the width of the peak in SNR with a finite value due to the interplay of the noise and the input signal.

In conclusion, we have investigated the coupled oscillator systems with time delay in the presence of the additive noise and the weak periodic signal. The system was presented as a model for the multiple perception of ambiguous or reversible figures, which is characterized by stochastic switchings in perception. We have showed SR in the system which implies that the stochastic switchings in multiple perception may be maximized at an optimum noise level. It would be interesting if our results can be tested in psychological systems. We have also investigated SR in the oscillator with time-delayed self-interaction which shows bistability of two limit-cycles.

This work was supported by the Ministry of Information and Communications, Korea.

*Electronic address: skim@etri.re.kr

[1] T. J. Walker, Science **166**, 891 (1969); M. K. McClintock, Nature (London) **229**, 244 (1971); H. Daido, Phys. Rev. Lett. **61**, 231 (1988); P. C. Matthews and S. H. Strogatz, Phys. Rev. Lett. **65**, 1701 (1990); E. Sismondo, Science **249**, 55 (1990); S. H. Strogatz, R. E. Mirollo, and P. C. Matthews, Phys. Rev. Lett. **68**, 2730 (1992); H. Daido, Phys. Rev. Lett. **73**, 760 (1994).

[2] H. Sompolinsky, D. Golomb, and D. Kleinfeld, Phys. Rev. A **43**, 6990 (1991).

[3] Y. Kuramoto and I. Nishikawa, J. Stat. Phys. **49**, 569 (1987); H. Daido, J. Phys. A **20**, L629 (1987); H. Sakaguchi, S. Shinomoto, and Y. Kuramoto, Prog. Theor. Phys. **77**, 1005 (1987); S. H. Strogatz and R. E. Mirollo, J. Phys. A **21**, L699 (1988).

[4] R. Eckhorn, R. Bauer, W. Jordan, M. Brosch, W. Kruse, M. Munk, and R. J. Reitboeck, Biol. Cybernet. **60**, 121 (1988); C. M. Gray, P. Konig, A. K. Engel, and W. Singer, Nature (London) **338**, 334 (1989).

[5] S. Kim, S. H. Park, and C. S. Ryu, Phys. Rev. Lett. **79**, 2911 (1997).

[6] A. Borsellino, A. De Marco, A. Allazetta, S. Rinesi, and B. Bartolini, Cybernetic **10**, 139 (1972); K. T. Brown, Am. J. Psychol. **68**, 358 (1955); A. Borsellino, F. Carlini, M. Riani, M. T. Tuccio, A. De Marco, P. Penengo, and A. Trabucco, Perception **11**, 263 (1982).

[7] H. Gang, T. Ditzinger, C. Z. Ning, and H. Haken, Phys. Rev. Lett. **71**, 807 (1993); T. Ditzinger and H. Haken, Biol. Cybernet. **63**, 453 (1990); M. Riani, F. Masulli, and E. Simonotto, Proc. SPIE Int. Soc. Opt. Eng. **1469**, 166 (1991).

[8] See, for example, *Proceedings of the NATO Advanced Research Workshop on Stochastic Resonance in Physics and Biology*, edited by F. Moss, A. Bulsara, and M. F. Shlesinger [J. Stat. Phys. **70**, 1 (1993)].

[9] S. Fauve and F. Heslot, Phys. Lett. A **97**, 5 (1983).

[10] B. McNamara, K. Wiesenfeld, and R. Roy, Phys. Rev. Lett. **60**, 2626 (1988).

[11] J. K. Douglass, L. Wilkens, E. Pantazelou, and F. Moss, Nature (London) **365**, 337 (1993); J. J. Collins, T. T. Imhoff, and P. Grigg, J. Neurophysiol. **76**, 642 (1996); B. J. Gluckman, T. I. Netoff, E. J. Neel, W. L. Ditto, M. L. Spano, and S. J. Schiff, Phys. Rev. Lett. **77**, 4098 (1996).

[12] J. Buhmann and K. Schulten, Biol. Cybernet. **56**, 313 (1987).

[13] S. Shinomoto and Y. Kuramoto, Prog. Theor. Phys. **75**, 1105 (1986).

[14] S. Kim, S. H. Park, and C. S. Ryu, Phys. Rev. E **54**, 6042 (1996); Phys. Rev. Lett. **78**, 1616 (1997); **78**, 1827 (1997).

[15] S. Kim, S. H. Park, and C. S. Ryu, ETRI J. **18**, 147 (1996).